Appendix A
Ray Tracing

Considering the paraxial approximation, a method can be established to propagate an optical ray in a system of refracting or reflecting surfaces. This makes it possible to measure the paraxial properties of the optical system, namely, focal points, principal points, and nodal points.

In Fig. A.1, the angles u and u' of inclination of the incident and refracted rays on a spherical surface of radius R are indicated, as well as the height y of the incident ray on the spherical surface. In the paraxial approximation, the height of the ray at the surface is measured along the segmented line passing through the vertex V of the surface, and the tangents of the angles are taken as the angles (in radians). Therefore,

$$u = -\frac{y}{s} \tag{A.1}$$

and

$$u' = -\frac{y}{s'}. \tag{A.2}$$

Multiplying Gauss' equation for the spherical surface of refraction [Eq. (1.21)] by the height y,

$$\frac{n'y}{s'} - \frac{ny}{s} = y\frac{n' - n}{R}. \tag{A.3}$$

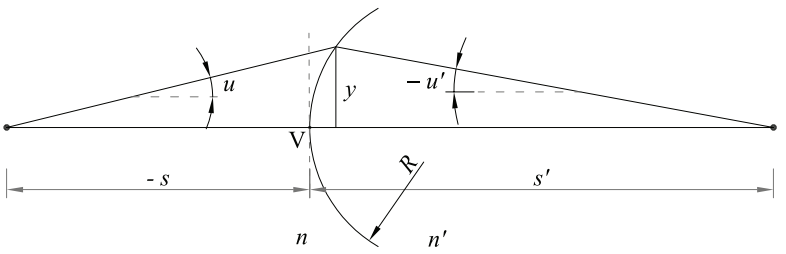

Figure A.1 Height and angles of inclination of a ray on a spherical refracting surface.

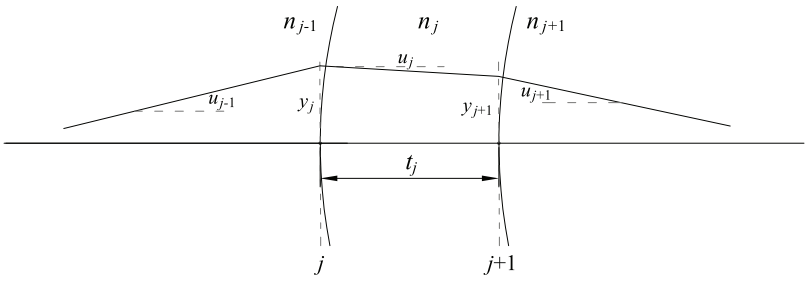

Figure A.2 Ray propagation on two surfaces.

And from Eqs. (A.1) and (A.2),

$$n'u' = nu - (n' - n)cy, \tag{A.4}$$

where $c = 1/R$ is the curvature of the surface. Equation (A.4) allows the angle of inclination of the ray to be propagated throughout the optical system.

To generalize propagation on various surfaces, let us consider two spherical surfaces of an optical system, as shown in Fig. A.2. The equation to propagate the angle from left to right of the jth surface becomes

$$n_j u_j = n_{j-1}u_{j-1} - P_j y_j, \tag{A.5}$$

where $P_j = (n_j - n_{j-1})c_j$ is the refractive power. Thus, $n'_{j-1} = n_j$ and $c_j = 1/R_j$.

On the other hand, the object for the $(j + 1)$th surface will be the image of the jth surface and the object and image distances are related by the separation or thickness t_j between the surfaces as

$$s_{j+1} = s'_j - t_j, \tag{A.6}$$

which is equal to

$$-\frac{y_{j+1}}{u_j} = -\frac{y_j}{u_j} - t_j, \tag{A.7}$$

i.e.,

$$y_{j+1} = y_j + \tau_j(n_j u_j), \tag{A.8}$$

where $\tau_j = t_j/n_j$ is the reduced thickness.

Thus, whereas the angle is propagated with Eq. (A.5) the height is propagated with Eq. (A.8). With these two equations, it can be seen how a ray evolves in an optical system with any number of refracting and/or reflecting surfaces. Equations (A.5) and (A.8) are the basis of the paraxial ray tracing *y-nu method* [1, 2].

Focal length of a set of lenses

From Eq. (A.5), the focal length of a set of refracting surfaces (lenses) can be determined. Suppose that there are M refracting surfaces. Then, for the M surfaces,

$$\begin{aligned} n_M u_M &= n_{M-1} u_{M-1} - P_M y_M \\ n_{M-1} u_{M-1} &= n_{M-2} u_{M-2} - P_{M-1} y_{M-1} \\ &\cdot \\ &\cdot \\ &\cdot \\ n_1 u_1 &= n_0 u_0 - P_1 y_1, \end{aligned} \tag{A.9}$$

and by adding these equations,

$$n_M u_M = n_0 u_0 - \sum_{j=1}^{M} P_j y_j. \tag{A.10}$$

The focal length of the system is determined when $s_0 = -\infty$, i.e., $u_0 = 0$ (and $y_1 = y_0$). Therefore,

$$f = -\frac{y_1}{u_M} \tag{A.11}$$

and

$$\frac{1}{f} = \frac{1}{n_M} \sum_{j=1}^{M} \frac{y_j}{y_1} P_j. \tag{A.12}$$

Focal length of a simple lens

As a result of Eq. (A.12), the focal length of a lens of thickness t immersed in air can be calculated. The geometry for calculating the focal length is illustrated in Fig. A.3. In this case, $M = 2$ and $n_0 = n_2 = 1$. Therefore, Eq. (A.12) is reduced to

$$\frac{1}{f} = P_1 + \frac{y_2}{y_1} P_2. \tag{A.13}$$

Using Eq. (A.8) for y_2,

$$\frac{1}{f} = P_1 + P_2 + P_2 \frac{\tau_1 (n_1 u_1)}{y_1} \tag{A.14}$$

and, with Eq. (A.5) for $n_1 u_1$,

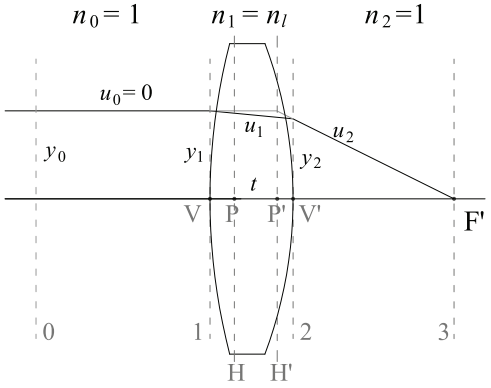

Figure A.3 Calculation of the focal length of a lens.

$$\frac{1}{f} = P_1 + P_2 - P_1 P_2 \frac{t}{n_l}, \tag{A.15}$$

where $n_l = n_1$ and $t = t_1$. This last equation is equivalent to

$$\frac{1}{f} = \frac{(n_l - 1)}{R_1} + \frac{(1 - n_l)}{R_2} - \frac{(n_l - 1)}{R_1}\frac{(1 - n_l)}{R_2}\frac{t}{n_l}. \tag{A.16}$$

Thus, the result for the focal length of a lens of thickness t given in Eq. (1.50) is obtained, i.e.,

$$\frac{1}{f} = (n_l - 1)\left(\frac{1}{R_1} - \frac{1}{R_2}\right) + \frac{(n_l - 1)^2}{R_1 R_2}\frac{t}{n_l}. \tag{A.17}$$

Principal planes

Principal planes can be located with respect to the vertices of the lens. Thus, the secondary principal plane is at a distance $\overline{\mathrm{V'P'}}$ from vertex V′, and the primary principal plane is at a distance $\overline{\mathrm{VP}}$ from vertex V. The distance between V′ and F′ is called the *back focal length*, $f_b = \overline{\mathrm{V'F'}}$, and the distance between V and F is called the *front focal length*, $f_f = \overline{\mathrm{VF}}$. Thus,

$$\overline{\mathrm{V'P'}} = f_b - f, \tag{A.18}$$

and because

$$\frac{y_1}{f} = \frac{y_2}{f_b},$$

from Eq. (A.8),

$$f_b = f\frac{y_1 + \tau_1(n_1 u_1)}{y_1} \tag{A.19}$$

and, with Eq. (A.5),

$$f_b = f\frac{y_1 + \tau_1(-P_1 y_1)}{y_1} \tag{A.20}$$

or

$$f_b = f - f\frac{tP_1}{n_l}. \tag{A.21}$$

Therefore,

$$\overline{\mathrm{V'P'}} = -f\frac{t(n_l - 1)}{n_l R_1}. \tag{A.22}$$

Note that $\overline{\mathrm{V'P'}}$ depends on the power of the first side of the lens. If it is zero ($r_1 = \infty$), then the secondary principal plane is at V′.

To determine $\overline{\mathrm{VP}}$, consider that the lens is rotated and the same procedure of the previous case is carried out, therefore,

$$\overline{\mathrm{VP}} = -f\frac{t(n_l - 1)}{n_l R_2}. \tag{A.23}$$

Focal length of a set of thin lenses

Approximating a set of lenses N by thin lenses (immersed in air), Eq. (A.12) is simplified as follows:

$$\frac{1}{f} = \sum_{k=1}^{N} \frac{y_k}{y_1}\frac{1}{f_k},$$

where y_k is the height of the ray in the kth lens and f_k is the focal length of the kth lens. For example, the focal length of two thin lenses at a distance d will be given by

$$\frac{1}{f} = \frac{1}{f_1} + \frac{y_2}{y_1}\frac{1}{f_2}.$$

Using Eq. (A.8) for y_2 and then Eq. (A.5) for $(n_1 u_1)$ leads to the known result

$$\frac{1}{f} = \frac{1}{f_1} + \frac{1}{f_2} - \frac{1}{f_1}\frac{1}{f_2}d.$$

References

[1] D. Malacara and Z. Malacara, *Handbook of Optical Design*, CRC Press, Boca Raton, Florida (2016).
[2] R. Ditteon, *Modern Geometrical Optics*, John Wiley & Sons, New York (1998).

Appendix B
Refractive Index

The refractive index in a medium measures the change in the speed of light in the medium with respect to the speed of light in a vacuum. Because the speed of light in a medium depends on the frequency ν, the refractive index also depends on the frequency. Denoting by n the refractive index, υ the speed of light in the medium, and c the speed of light in a vacuum, the refractive index is given by the equation

$$n(\nu) = \frac{c}{\upsilon(\nu)}, \tag{B.1}$$

which is also known as the *dispersion relation*.

From the microscopic point of view, in a classical approximation, the speed change occurs due to the phase change of the electromagnetic wave reemitted by the induced electric dipoles that make up the medium with respect to the incident electromagnetic wave (of speed c).

Refractive index in dielectric materials

To obtain a first model of the refractive index in a dielectric medium, it is initially assumed that the medium in the presence of an external electric field is composed of N induced dipoles of the type $\mathbf{p} = -e\mathbf{r}$ (electron attached to an atom) per unit volume. Because the dipole is surrounded by other dipoles, in the presence of a harmonic electromagnetic wave of amplitude $\mathbf{E}_0$ and frequency ν, the dipole will oscillate similarly to a driven damped harmonic oscillator. Thus, if

$$\mathbf{E} = \mathbf{E}_0 e^{-i\omega t} \tag{B.2}$$

represents the harmonic wave, with $\omega = 2\pi\nu$, the electric force on the charge e will be

$$\mathbf{F} = -e\mathbf{E}. \tag{B.3}$$

The charge displacement vector e satisfies

$$m_e \frac{d^2\mathbf{r}}{dt^2} + m_e\gamma \frac{d\mathbf{r}}{dt} + k\mathbf{r} = -e\mathbf{E}_0 e^{-i\omega t}, \tag{B.4}$$

where m_e is the mass of the charge e, γ is the damping constant (due to the presence of the other dipoles), and k is the constant that explains the force that holds the charge together for the atom.

In steady state, the response of the dipole will be

$$\mathbf{r} = \mathbf{r}_0 e^{-i(\omega t+\delta)}; \tag{B.5}$$

i.e., it will oscillate with the same frequency as the incident wave, but with an offset δ. By inserting Eq. (B.5) in Eq. (B.4),

$$\mathbf{r}_0 = \frac{-e\mathbf{E}_0/m_e}{(\omega_0^2 - \omega^2) - i\gamma\omega} e^{i\delta}, \tag{B.6}$$

with $\omega_0^2 = k/m_e$. With this result,

$$\mathbf{r} = -\frac{(e/m_e)}{(\omega_0^2 - \omega^2) - i\gamma\omega}\mathbf{E}, \tag{B.7}$$

and the induced electric polarization vector $\mathbf{P} = -Ne\mathbf{r}$ is

$$\mathbf{P} = \frac{Ne^2/m_e}{(\omega_0^2 - \omega^2) - i\gamma\omega}\mathbf{E}. \tag{B.8}$$

Thus, the macroscopic effect of the electromagnetic wave incident on the medium is a polarization vector, which is proportional to $\mathbf{E}$. In general, the equation above can be written as

$$\mathbf{P} = \epsilon_0\chi\mathbf{E}, \tag{B.9}$$

where ϵ_0 is the permittivity of the vacuum (a constant) and χ is the electrical susceptibility of the medium, which measures the degree of proportionality with $\mathbf{E}$ and is defined as $\chi = \epsilon/\epsilon_0 - 1$, where ϵ is the permittivity of the medium.

On the other hand, in dielectric (nonmagnetic) media, there is the magnetic polarization vector, $\mathbf{M} = 0$; the electric current density vector, $\mathbf{J} = 0$; and the free charge density, $\rho = 0$. Thus, Maxwell's equations for the medium have the form [1]

$$\nabla \times \mathbf{E} = -\mu_0 \frac{\partial \mathbf{H}}{\partial t}, \tag{B.10}$$

$$\nabla \times \mathbf{H} = \epsilon_0 \frac{\partial \mathbf{E}}{\partial t} + \frac{\partial \mathbf{P}}{\partial t}, \tag{B.11}$$

$$\nabla \cdot \mathbf{E} = -\frac{\nabla \cdot \mathbf{P}}{\epsilon_0}, \tag{B.12}$$

$$\nabla \cdot \mathbf{H} = 0, \tag{B.13}$$

where $\mathbf{H}$ is the magnetic vector and μ_0 is the vacuum permeability.

The wave equation that results from taking $\nabla \times (\nabla \times \mathbf{E}) = -\mu_0 \partial(\nabla \times \mathbf{H})/\partial t$, and also using Eqs. (B.11) and (B.9), is

$$\nabla(\nabla \cdot \mathbf{E}) - \nabla^2 \mathbf{E} = -\mu_0 \epsilon_0 (1 + \chi) \frac{\partial^2 \mathbf{E}}{\partial t^2}. \tag{B.14}$$

Isotropic media

A medium is isotropic if its physical properties do not depend on direction. In particular, in optics, a medium is said to be isotropic if the refractive index does not depend on the direction of propagation of light. This implies that in Eq. (B.9) the electrical susceptibility is described by a scalar. Otherwise, in an anisotropic medium (in which the refractive index depends on the direction), the electrical susceptibility is described by a tensor (3×3 matrix).

Assuming that the electrical medium is isotropic, then in Eq. (B.12),

$$\nabla \cdot (\epsilon_0 \mathbf{E} + \chi \epsilon_0 \mathbf{E}) = (1 + \chi) \nabla \cdot \mathbf{E} = 0, \tag{B.15}$$

which implies that $\nabla \cdot \mathbf{E} = 0$, since $\chi \geq 0$. Therefore, the wave equation for the isotropic dielectric medium is given by

$$\nabla^2 \mathbf{E} = \mu_0 \epsilon_0 (1 + \chi) \frac{\partial^2 \mathbf{E}}{\partial t^2}; \tag{B.16}$$

thus, the speed of light in the medium is determined from

$$\frac{1}{\upsilon^2} = \mu_0 \epsilon_0 (1 + \chi). \tag{B.17}$$

Because $c^2 = 1/\mu_0 \epsilon_0$, the refractive index turns out to be

$$n^2 = 1 + \chi. \tag{B.18}$$

And with the result obtained for the medium of the example given by Eq. (B.8), then

$$n^2 = 1 + \frac{Ne^2}{m_e \epsilon_0} \frac{1}{[(\omega_0^2 - \omega^2) - i\gamma\omega]}. \tag{B.19}$$

Starting from the previous result, a generalization of the medium is achieved by assuming that instead of a single type of electric dipole there are M types of dipoles [2]. If N_j is the volume density of the jth type of dipole, then

$$g_j = \frac{N_j}{N} \tag{B.20}$$

is the fraction of jth type of dipole and $\sum_{j=1}^{M} g_j = 1$. With this in mind, the refractive index can then be written in a general form as

$$n^2 = 1 + \frac{Ne^2}{m_e \epsilon_0} \sum_{j=1}^{M} \frac{g_j}{[(\omega_{0j}^2 - \omega^2) - i\gamma_j \omega]}, \tag{B.21}$$

where there are now several eigenfrequencies ω_{0j} and damping constants γ_j corresponding to each type of dipole.

According to Eq. (B.21), the refractive index is a quantity of complex variable, i.e., $n = n_R + in_I$. Taking the real and imaginary parts of the square of the refractive index,

$$n_R^2 - n_I^2 = 1 + \frac{Ne^2}{m_e \epsilon_0} \sum_{j=1}^{M} \frac{(\omega_{0j}^2 - \omega^2)}{[(\omega_{0j}^2 - \omega^2)^2 + \gamma_j^2 \omega^2]} g_j \tag{B.22}$$

and

$$2n_R n_I = \frac{Ne^2}{m_e \epsilon_0} \sum_{j=1}^{M} \frac{\gamma_j \omega}{[(\omega_{0j}^2 - \omega^2)^2 + \gamma_j^2 \omega^2]} g_j. \tag{B.23}$$

Although this model requires adjustments to be applied in real cases, it allows us to see the dependence of the refractive index on frequency. On the other hand, it shows that the refractive index has two components: a real one n_R, with which refraction can be explained, and an imaginary one n_I, which represents the absorption in the medium.

The general behavior of n_R and n_I through Eqs. (B.22) and (B.23) is shown in Fig. B.1 for two resonance frequencies: ω_{01} and ω_{02}. The damping constants γ_j are usually small compared with the respective resonance frequencies ω_{0j}. When $\omega \approx \omega_{0j}$, the imaginary part of the refractive index takes relevant values that give rise to absorption bands. When ω moves away from the resonant frequencies, the imaginary part of the index of refraction is practically zero, and the real part of the index of refraction increases with frequency. This behavior is called *normal dispersion*. When the real part of the refractive index decreases with frequency, it is called *anomalous dispersion* (region where absorption occurs).

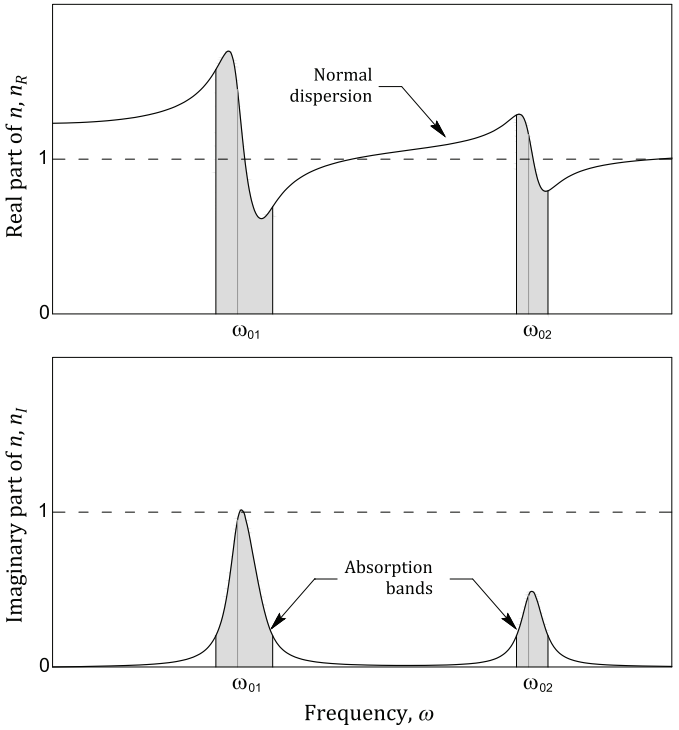

Figure B.1 General behavior of the real and imaginary parts of the refractive index according to Eqs. (B.22) and (B.23).

The speed of light in the medium can also be given in terms of the permittivity ϵ and the permeability μ of the medium (which also depend on the frequency of the electromagnetic wave incident on the medium); i.e.,

$$\frac{1}{v^2} = \mu\epsilon. \tag{B.24}$$

Therefore, the refractive index is

$$n^2 = \frac{\mu\epsilon}{\mu_0\epsilon_0}. \tag{B.25}$$

For nonmagnetic materials, the $\mu \approx \mu_0$ approximation can be made, and in this case the refractive index can be calculated as

$$n = \sqrt{\frac{\epsilon}{\epsilon_0}}. \tag{B.26}$$

References

[1] G. R. Fowles, *Introduction to Modern Optics*, 2nd ed., Dover Publications, Mineola, New York (1989).
[2] E. Hecht, *Optics*, Global Edition, 5th ed., Pearson, Harlow, England (2017).

Appendix C
Optical Glasses

The refractive index varies with the speed of the electromagnetic wave in the medium, as shown in Appendix B. In turn, the speed depends on the frequency of the wave (or the wavelength in a vacuum, for $\lambda = c/\nu$, where ν is the wave frequency). As a function of wavelength, away from resonance frequencies, the refractive index decreases with increasing wavelength; near resonance frequencies, where absorption occurs, the refractive index increases. This can be understood by the dispersion relation obtained in Eq. (B.21). In practice, the dispersion relation for each medium is obtained empirically as a function of the wavelength. For example, the glass used for microscope slides, *soda lime silica*, can be characterized in the visible range by the relationship obtained by Rubin [1]:

$$n = 1.5130 - 0.003169\lambda^2 + 0.003962\lambda^{-2}. \tag{C.1}$$

Another way to characterize optical glasses is by the refractive index at three wavelengths corresponding to two spectral lines of hydrogen and one spectral line of helium, as shown in Table C.1.

With these spectral lines, the visible range is covered. These are used for analysis of chromatic aberrations. The indices of the corresponding colors are indicated by n_F, n_d, and n_C. On the other hand, a measure of chromatic dispersion is given by

$$V = \frac{n_d - 1}{n_F - n_C}, \tag{C.2}$$

which is called the *Abbe number*. Usually, when the refractive index of a medium is said to be n, by default (unless otherwise stated) this value corresponds to the index n_d.

Optical glasses are made from SiO_2 and a combination of light metals (*crown* glass) or heavy metals (*flint* glass), with which it is possible to set the refractive indices and the desired Abbe number.

Table C.1 Spectral lines to characterize optical glasses.

Line	Wavelength	Element	Color
F	486.13	H	blue
d	587.56	He	yellow
C	656.27	H	red

An *Abbe diagram* plots the refractive index n_d versus the Abbe number for a range of different optical glasses, as shown in Fig. C.1. Each glass is identified by a labeled point on the graph n_d versus V. Thus, the glasses used in the manufacture of optical elements (lenses, prisms, mirrors, etc.) are identified with the name of the glass (and not with the refractive index).

For example, consider an achromatic doublet manufactured by a commercial company. The catalog says that the first lens is made of BK7 glass and the second is made of SF5 glass. The difference in glasses is intended to correct axial chromatic aberration (for blue and red colors). It can seen in Fig. C.1 that the index n_d for BK7 glass is 1.52 ± 0.05 (1.5168) and its Abbe number is 64.0 ± 0.5 (64.17), and the index n_d for SF5 glass is 1.68 ± 0.05 (1.6727) and its Abbe number is 32.0 ± 0.5 (32.21).

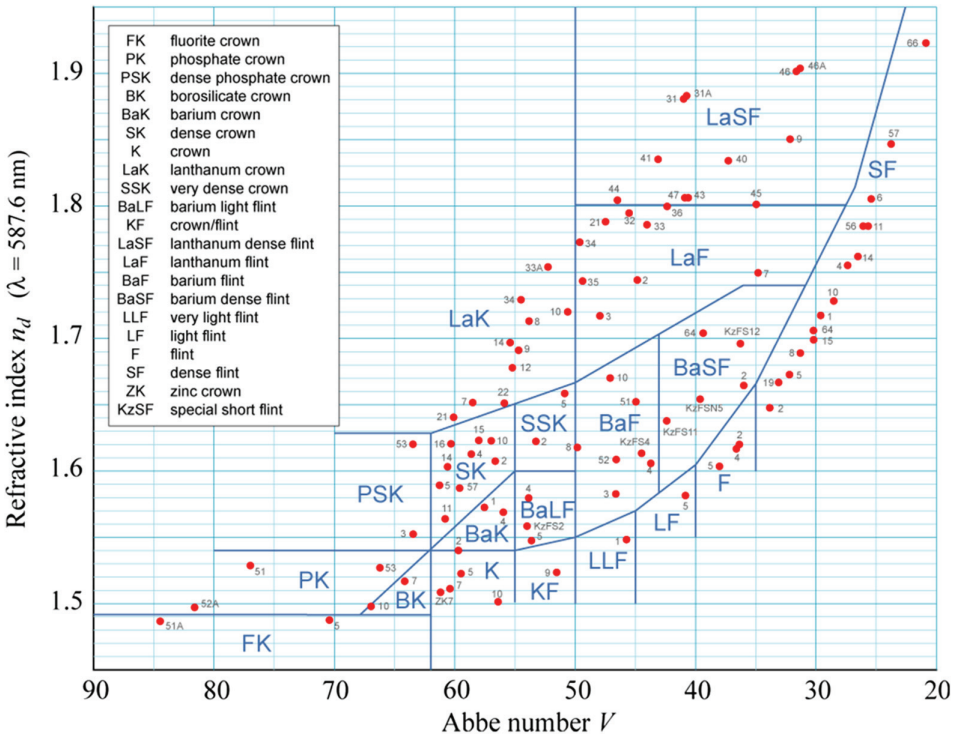

Figure C.1 Abbe diagram of optical glasses. Reprinted from [2] with permission granted by the GNU Free Documentation License.

References

[1] M. Rubin, "Optical properties of soda lime silica glasses," *Sol. Energy Mater.* **12**(4), 275–288 (1985).
[2] B. Mellish, "Abbe-diagram," Wikimedia Commons, https://commons.wikimedia.org/wiki/File:Abbe-diagram.svg, accessed November 7, 2022.

Appendix D
Chromatic Aberrations

Chapter 1 deals with imaging systems for a single wavelength. When the light coming from the object is polychromatic, the parameters that depend on the refractive index change according to the color of the light; e.g., the focal length of a lens, see Eq. (1.50), and the position of the principal planes, see Eqs. (1.51) and (1.52). Consequently, for each color there will be an image of a different size and in a different axial position.

Let us consider the three wavelengths shown in Table D.1 with which optical glasses are characterized.

Denoting the focal lengths for these colors as f_F, f_d, and f_C, the equations for locating the image in each case are

$$\frac{1}{s'_F} - \frac{1}{s_F} = \frac{1}{f_F}, \tag{D.1}$$

$$\frac{1}{s'_d} - \frac{1}{s_d} = \frac{1}{f_d}, \tag{D.2}$$

$$\frac{1}{s'_C} - \frac{1}{s_C} = \frac{1}{f_C}. \tag{D.3}$$

In the case of a lens, the distance between the object and the first surface of the lens is the same in all three cases, i.e., $s_F - (\overline{\mathrm{VP}})_F = s_d - (\overline{\mathrm{VP}})_d = s_C - (\overline{\mathrm{VP}})_C$. The former also implies that, in general, the distance of the object is different depending on the color. For the image, the situation is a bit more complex, since in general $s'_F + (\overline{\mathrm{V'P'}})_F \neq s'_d + (\overline{\mathrm{V'P'}})_d \neq s'_C + (\overline{\mathrm{V'P'}})_C$.

Table D.1 Spectral lines to characterize optical glasses.

Line	Wavelength (nm)	Element	Color
F	486.13	H	blue
d	587.56	He	yellow
C	656.27	H	red

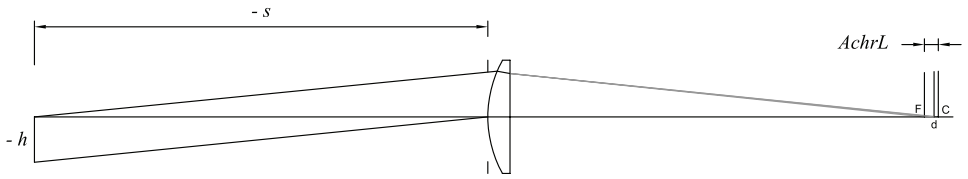

Figure D.1 Axial chromatic aberration in a positive lens.

The axial difference between the positions of the images corresponding to the spectral lines F and C,

$$\begin{aligned} AchrL &= (s'_F + (\overline{\mathrm{V'P'}})_F) - (s'_C + (\overline{\mathrm{V'P'}})_C) \\ &= (s'_F - s'_C) + ((\overline{\mathrm{V'P'}})_F - (\overline{\mathrm{V'P'}})_C), \end{aligned} \tag{D.4}$$

is called the *axial chromatic aberration*. For example, Fig. D.1 shows the position of the images for the spectral lines F, d, and C for a lens of focal length $f_d = 50$ mm ($R_1 = 25.84$ mm, $R_2 = \infty$, thickness $t = 4.5$ mm; glass BK7) when the object is at $s_d = -100$ mm, which gives a magnification $m_t = -1$ for the spectral line d. In this example, the primary principal plane is at the vertex of the first surface; thus, $s_d = s_F = s_C$. The parameters for this example are summarized in Table D.2. All distances (except wavelength) are given in millimeters. From these data it follows that the axial chromatic aberration is $AchrL = -3.05$ mm.

Suppose that the object is a point and the system is free of primary monochromatic aberrations. Then, for the spectral lines F, d, and C, there are three image points located at $s'_F = 94.67$ mm, $s'_d = 96.77$ mm, and $s'_C = 97.73$ mm, respectively. Where should the image plane be located? If it is set at s'_F, there will be a blue dot in focus, but the yellow and red images will be out of focus. Analogous situations occur if the image plane is located at s'_d and s'_C. However, in the middle of the blue and red images there will be a circle of least confusion, and this will be the place where the best image can be seen. By focusing on s'_F, there will be a red dot larger than the yellow dot. On the other hand, focusing on s'_C will result in a blue dot that is larger than the yellow dot. This means that the edge of the image of a polychromatic object

Table D.2 Parameters of a positive lens and the image according to the spectral lines to characterize optical lenses when the object is at −100 mm from the primary principal plane.

Line	λ(nm)	f	$\overline{\mathrm{V'P'}}$	s'	m_t
F	486.13	49.46	−3.21	94.67	−0.9788
d	587.56	50.00	−3.23	96.77	1
C	656.27	50.24	−3.23	97.73	−1.0097

obtained with a simple lens (like the example shown in Fig. D.1) looks red from a distance s'_F, whereas it looks blue from a distance s'_C.

Magnification also depends on the wavelength in an image plane; there will be a superposition of images of different colors and sizes (one in focus and others out of focus). If $h'_F = m_{tF}h$ and $h'_C = m_{tC}h$ are the heights of the images, the difference

$$AchrT = h'_F - h'_C \tag{D.5}$$

is defined as *transverse chromatic aberration*.

With a negative lens, the order in which the images are placed for each color is opposite to that of the positive lens. This can be seen with an example similar to the positive lens. For a lens of focal length $f_d = -50$ mm ($R_1 = -25.84$ mm, $R_2 = \infty$, thickness $t = 3.5$ mm; BK7 glass) when the object is at $s_d = -100$ mm, the virtual image for blue is closer to the lens than the image for red (and the image for yellow in between; Fig. D.2).

The values of the distances are shown in Table D.3. The chromatic aberration in this case is $AchrL = 0.36$ mm.

Achromatic doublet

The union of two lenses results in a single lens called a *doublet achromatic*. This assumes that the radius of curvature of the posterior face of the first lens must be equal to the radius of curvature of the anterior face of the second lens, i.e., $R_{12} = R_{21}$ (Fig. D.3).

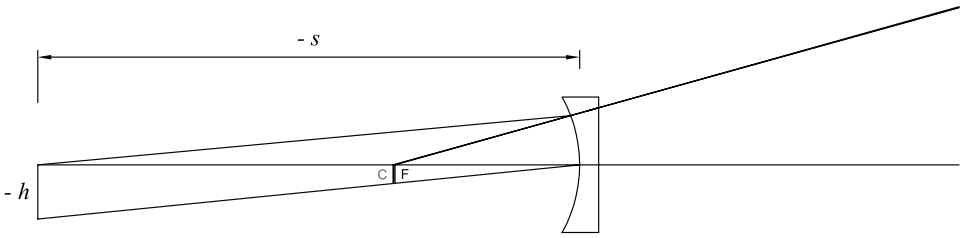

Figure D.2 Axial chromatic aberration in a negative lens.

Table D.3 Parameters of a negative lens and the virtual image according to the spectral lines to characterize optical lenses when the object is −100 mm from the primary principal plane.

Line	λ(nm)	f	$\overline{V'P'}$	s'	m_t
F	486.13	−49.46	−2.30	−35.39	0.3309
d	587.56	−50.00	−2.31	−35.64	0.3333
C	656.27	−50.24	−2.31	−35.75	0.3344

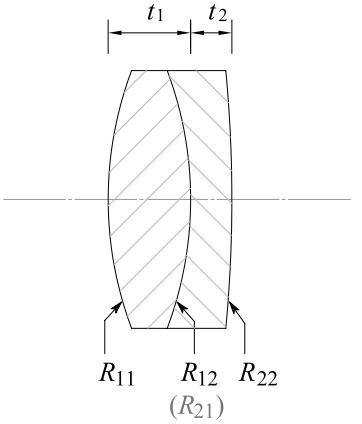

Figure D.3 Achromatic doublet.

Suppose we want to obtain an achromatic doublet of focal length f_d. From the thin lens approximation, the focal length of the combination of two thin lenses [Eq. (1.53)] will be

$$\frac{1}{f_d} = \frac{1}{f_{1d}} + \frac{1}{f_{2d}}, \tag{D.6}$$

since the separation between the lenses is zero. For each lens,

$$\frac{1}{f_{1d}} = P_{1d} = (n_{1d} - 1)\left(\frac{1}{R_{11}} - \frac{1}{R_{12}}\right) = (n_{1d} - 1)\kappa_1 \tag{D.7}$$

and

$$\frac{1}{f_{2d}} = P_{2d} = (n_{2d} - 1)\left(\frac{1}{R_{21}} - \frac{1}{R_{22}}\right) = (n_{2d} - 1)\kappa_2. \tag{D.8}$$

In Eqs. (D.7) and (D.8), the factors κ_1 and κ_2 have been introduced for the difference in curvatures. Thus, the power of the achromatic doublet in the approximation of thin lenses is

$$P = (n_{1d} - 1)\kappa_1 + (n_{2d} - 1)\kappa_2. \tag{D.9}$$

The achromatic doublet implies that the power is constant as the wavelength changes in the neighborhood of $\lambda = 587.56$ nm, i.e.,

$$\left(\frac{\partial P}{\partial \lambda}\right)_d = 0. \tag{D.10}$$

In other words,

$$\kappa_1 \frac{\partial n_1}{\partial \lambda} + \kappa_2 \frac{\partial n_2}{\partial \lambda} = 0. \tag{D.11}$$

By approximating the variation of the refractive index with $n_F - n_C$ and the variation of the wavelength with $\lambda_F - \lambda_C$,

$$\kappa_1 \frac{n_{1F} - n_{1C}}{\lambda_F - \lambda_C} - \kappa_2 \frac{n_{2F} - n_{2C}}{\lambda_F - \lambda_C} = 0. \tag{D.12}$$

By multiplying and dividing each addend by $(n_{1d} - 1)$ and $(n_{2d} - 1)$, respectively, to introduce the Abbe number,

$$\begin{aligned} 0 &= \kappa_1 \frac{(n_{1F} - n_{1C})}{(n_{1d} - 1)} \frac{(n_{1d} - 1)}{(\lambda_F - \lambda_C)} - \kappa_2 \frac{(n_{2F} - n_{2C})}{(n_{2d} - 1)} \frac{(n_{2d} - 1)}{(\lambda_F - \lambda_C)} \\ &= \kappa_1 \frac{(n_{1d} - 1)}{(\lambda_F - \lambda_C) V_1} - \kappa_2 \frac{(n_{2d} - 1)}{(\lambda_F - \lambda_C) V_2}. \end{aligned} \tag{D.13}$$

By eliminating the common factor from the denominator and using the definition of power for each lens, i.e., Eqs. (D.7) and (D.8),

$$\frac{P_{2d}}{V_2} = -\frac{P_{1d}}{V_1}. \tag{D.14}$$

This equation and Eq. (D.6) in the form of powers $P_d = P_{1d} + P_{2d}$ allow us to write the power of each lens as a function of the Abbe numbers of each glass and the power of the achromatic doublet, as follows,

$$P_{1d} = P_d \frac{-V_1}{V_2 - V_1} \tag{D.15}$$

and

$$P_{2d} = P_d \frac{V_2}{V_2 - V_1}. \tag{D.16}$$

After this, the curvature factors are obtained:

$$\kappa_1 = \frac{P_{1d}}{n_{1d} - 1} \tag{D.17}$$

and

$$\kappa_2 = \frac{P_{2d}}{n_{2d} - 1}. \tag{D.18}$$

To finalize the design of the doublet, the radii of curvature of the lenses must be determined. A very common design proposes that the first lens

be an equiconvex lens of crown glass [1]. Thus, the radii satisfy the following relations:

$$R_{11} = -R_{12}, \quad R_{12} = R_{21} \quad \text{and} \quad R_{22} = \frac{R_{12}}{1 - \kappa_2 R_{12}}. \tag{D.19}$$

Example: achromatic doublet

Suppose an achromatic doublet of focal length $f_d = 50$ mm is desired. The power would be $P = 20$ D. Using the glasses LAKN22 for the first lens and SFL6 for the second lens (Appendix C) and Eqs. (D.15–D.18), together with the definition of the curvature factors, leads to the results for the radii of curvature shown in Table D.4.

To have real lenses, we need to assign a thickness to each lens, e.g., 8 mm for the first lens and 4 mm for the second. The (real) achromatic doublet is summarized in Table D.5. With these parameters, the focal length for the spectral line d becomes $f_d = 50.85$ mm.

To see the improvement in imaging, compare the image with this doublet and image with the single lens of Fig. D.1 by placing an object at $s_d = -101.7$ mm from the doublet (such that the magnification is again $m_t = -1$ for the spectral line d). The parameters for the three spectral lines are shown in Table D.6. The axial chromatic aberration is $AchrL = -0.19$ mm, i.e., only

Table D.4 Design parameters of an achromatic doublet in the thin lens approximation.

P(D)	20
V_1	55.89
V_2	25.39
n_{1d}	1.6511
n_{2d}	1.8051
κ_1(D)	56.29
κ_2(D)	−20.68
R_{11}(mm)	35.52
R_{22}(mm)	−133.97

Table D.5 Achromatic doublet. The units of radius and thickness are given in millimeters.

Surface	Radius	Thickness	Index
1	35.52	8	LAKN22
2	−35.52	4	SFL6
3	−133.97		

Table D.6 Parameters of an achromatic doublet and the image along the spectral lines to characterize optical lenses when the object is at −101.7 mm from the primary principal plane for the spectral line d.

Line	λ(nm)	f	$\overline{VP}$	$\overline{V'P'}$	s'	m_t
F	486.13	50.83	1.05	−6.13	95.54	−1.0002
d	587.56	50.85	1.10	−6.13	95.57	1
C	656.27	50.90	1.12	−6.14	95.73	−1.0014

6% of the aberration obtained with the simple lens. On the other hand, the magnification of each color varies very little, which makes transverse chromatic aberration negligible. Thus, with the achromatic doublet, a high-quality image is achieved.

Although the original design calls for a focal length of 50 mm on the d line, the proposed actual doublet has a slightly higher value. With a small adjustment in the radii of curvature of the first lens, the desired value can be obtained (e.g., with $R_{11} = -R_{12} = 34.7$ mm, $f_d = 50.01$ mm is obtained).

Achromatic doublets are very common in imaging systems because, in addition to producing good-quality images, they also reduce spherical aberration. Another possible solution to reduce chromatic aberration is to design two lenses of the same glass separated by the distance $[(f_{1d} + f_{2d})/2]$. This can be consulted in [2].

References

[1] R. Ditteon, *Modern Geometrical Optics*, John Wiley & Sons, New York (1998).

[2] D. Malacara and Z. Malacara, *Handbook of Optical Design*, CRC Press, Boca Raton, Florida (2016).

Appendix E
Prisms

A prism is an optical element with flat faces of which at least two are mirror-polished and inclined toward each other, such that light can be reflected or transmitted by them. Prisms used to reflect light do so by total internal reflection on one or more of their faces and serve to change the orientation of images in an optical system or the direction of light propagation [1]. On the other hand, prisms that make use of refraction are used as elements to scatter light and to measure the change of the refractive index in a medium (prism) with the wavelength or spectral components of a light source.

Reflecting prisms

Figure E.1 shows images of reflecting prisms: (a) right-angle prism, (b) Porro prism, (c) pentaprism, and (d) Amici prism. In these prisms, a beam of light falls on one of the faces and the transmitted beam must undergo at least one total internal reflection. Right-angle and Porro prisms are geometrically the same; the difference is their orientations with respect to the direction of light. Assuming that light falls from left to right, the path followed by light in this type of prism is illustrated in Fig. E.2. To see how the orientation changes in

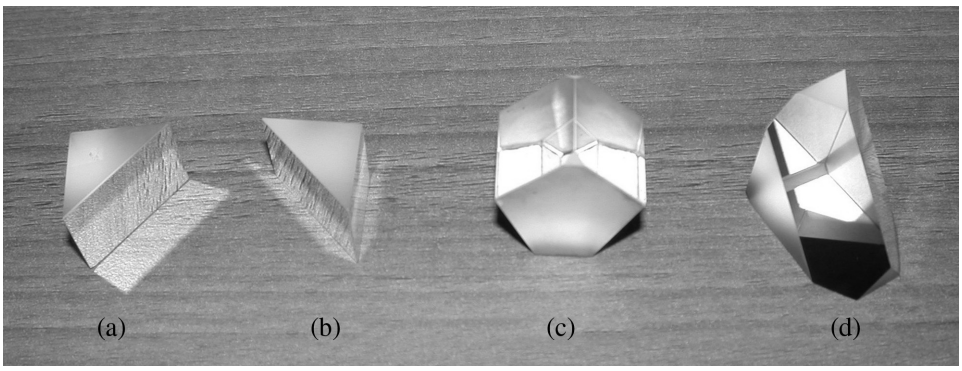

Figure E.1 Reflecting prisms: (a) right-angle prism, (b) Porro prism, (c) pentaprism, and (d) Amici prism.

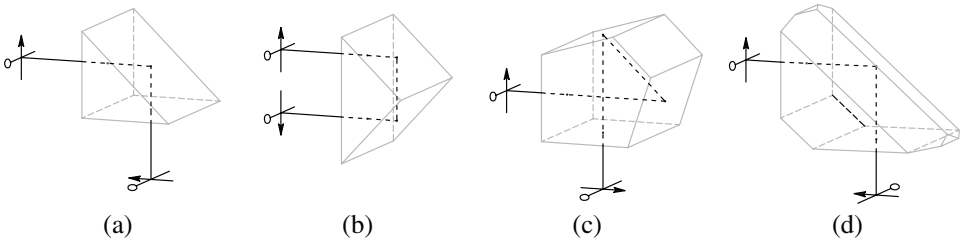

Figure E.2 Direction that light follows when reflected internally in the (a) right-angle prism, (b) Porro prism, (c) pentaprism, and (d) Amici prism.

the image, a couple of symbols are included in the incident beam: an arrow pointing up and a circle to the left (out of the plane of the paper). Light is also assumed to propagate toward the observer. After the reflection on the diagonal face, the right-angle prism deflects the light 90°, inverts the arrow, and keeps the orientation of the circle, such that when looking at the arrow pointing up again (with a rotation of 180°), the circle faces right (reverses from left to right). The Porro prism reflects light parallel to the incident beam, rotates the arrow twice, and maintains the orientation of the circle, so that when looking at the arrow, the circle stays to the left (does not change orientation*). The pentaprism deflects light 90° and does not change orientation. The Amici prism deflects the light 90°, reverses the arrow, and reflects the circle twice off the roof of the prism, changing its orientation in such a way that when looking again at the arrow pointing up, the circle is on the left (it does not change orientation).

A configuration that allows the direction of light propagation to be maintained with an inversion of the image (central symmetry) is achieved by combining two Porro prisms, as shown in Fig. E.3. This system of prisms is usually used in binoculars (terrestrial telescope) in which the image is seen from the front. The Amici prism is also often used in eyepieces to correct image inversion in spotting scopes. The pentaprism is often used in range finders and alignment instruments in topographic surveying. A variant of the pentaprism results from changing one of the flat reflecting faces to a roof-shaped face (similar to the Amici prism); this is usually used in reflex-type cameras.

Another very useful prism is the Dove prism, the configuration of which is shown in Fig. E.4. An incident ray parallel to the base is refracted at the first face, then reflected internally at the base (midpoint), and finally emerges parallel to the incident ray by reversing the arrow. This prism must be used with collimated light and has the following property: if the prism is rotated about the optical axis (incident beam) by a certain angle, the image is rotated by twice that angle. For example, in some slit lamps (ophthalmic instruments),

*The orientation between the arrow and circle.

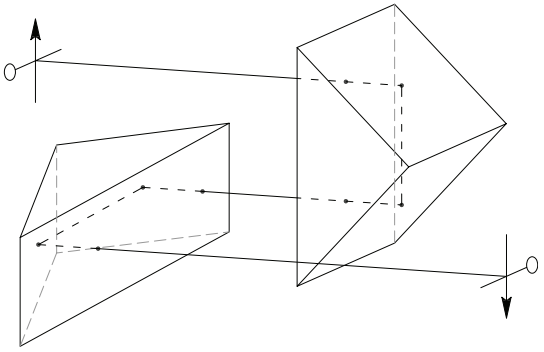

Figure E.3 A combination of two Porro prisms to invert the image (central symmetry with respect to a point on the optical axis) and maintain the direction of propagation.

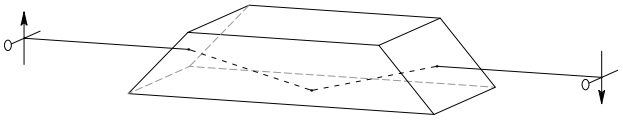

Figure E.4 Dove prism.

the Dove prism is placed between the two lenses of a confocal system that projects a line of light onto the surface of the cornea. To observe corneal astigmatism, it is common to rotate the line by an angle of 90°, which is done by rotating the cylindrical support that contains the Dove prism by an angle 45°. It is very convenient for an instrument operator to rotate the beamline.

Beamsplitter cubes

Another widely used prism configuration is the beamsplitter cube formed by two right prisms joined by their diagonal faces to divide an incident beam into transmitted and reflected beams [Fig. E.5(a)]. One of the faces of the diagonals is covered with a reflective film (semi-mirror), and the diagonals are

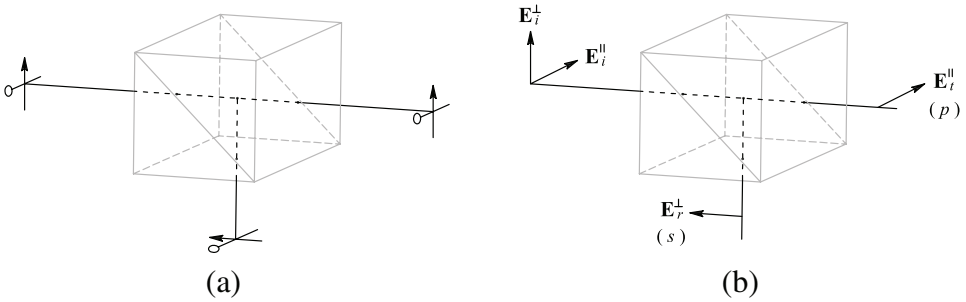

Figure E.5 (a) Nonpolarizing and (b) polarizing beamsplitter cubes.

joined using an optical adhesive. The thickness of the reflective film determines the percentages of light reflected and transmitted on the diagonal. The refractive index of the optical adhesive must be close to that of the prisms to avoid unwanted reflections. One of the most common cubes transmits 50% and reflects 50% of the light.

The cubes are also designed to separate an unpolarized beam into a transmitted beam with polarization *p* and a reflected beam with polarization *s*, as shown in Fig. E.5(b). The diagonal of one of the prisms is covered with a dielectric film or metal–dielectric mixture. When the incident beam reaches the film, the beam with polarization parallel to the plane of incidence (*p*) is transmitted, while the beam with polarization orthogonal to the plane of incidence (*s*) is reflected.

Refracting prisms

Prisms can also be used to analyze the spectral components (in wavelength or frequency) of a light source. Because the refractive index is a function of wavelength, a polychromatic light beam refracts into multiple beams depending on its wavelength. This physical separation of the refracted rays allows the light spectrum to be measured. To determine the deviation of the refracted ray as a function of the refractive index, let us consider the refraction of a ray at two faces of a prism that form an angle α, as shown in Fig. E.6.

Suppose that the prism is immersed in a medium of index n_1 and that the index of refraction of the prism for the beam considered is n_2. Snell's law on both sides would be

$$n_1 \sin\theta_{i1} = n_2 \sin\theta_{t1} \tag{E.1}$$

and

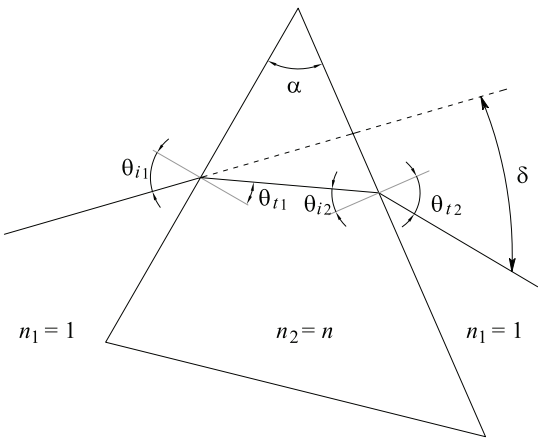

Figure E.6 Refraction of a beam at two faces of a prism.

$$n_2 \sin\theta_{i2} = n_1 \sin\theta_{t2}. \tag{E.2}$$

From the geometry of Fig. E.6, $\alpha = \theta_{t1} + \theta_{i2}$. Changing θ_{i2} to $\alpha - \theta_{t1}$ in Eq. (E.2),

$$\sin\theta_{t2} = \frac{n_2}{n_1}(\sin\alpha\cos\theta_{t1} - \cos\alpha\sin\theta_{t1}), \tag{E.3}$$

which is equal to

$$\sin\theta_{t2} = \sin\alpha\sqrt{\left(\frac{n_2}{n_1}\right)^2 - \sin^2\theta_{i1}} - \cos\alpha\sin\theta_{i1}. \tag{E.4}$$

If $n_1 = 1$ and $n_2 = n$, the index of refraction of the prism for a ray of a certain wavelength is given by

$$n^2 = \sin^2\theta_{i1} + \frac{(\sin\theta_{t2} + \sin\theta_{i1}\cos\alpha)^2}{\sin^2\alpha}. \tag{E.5}$$

Using a prism characterized in its refractive indices according to wavelength, we can measure the light spectrum of a source by observing the position of the refracted rays on a length scale. One configuration used in prism spectrometers is based on the minimum value of the angle $\delta = \theta_{i1} + \theta_{t2} - \alpha$, which measures the deviation of the refracted ray leaving the prism with respect to the ray that is incident on the prism. The minimum of δ occurs when $\theta_{t2} = \theta_{i1} = \theta_{\min}$ [2]. In this case,

$$n = \frac{\sin\theta_{\min}\sqrt{2(1+\cos\alpha)}}{\sin\alpha}, \tag{E.6}$$

and because $\theta_{\min} = (\delta_{\min} + \alpha)/2$, then

$$n = \frac{\sin[(\delta_{\min} + \alpha)/2]}{\sin(\alpha/2)}. \tag{E.7}$$

In particular, if the prism is constructed as an isosceles triangle, where α is the angle between the two equal sides, the ray refracted inside the prism will be parallel to the other side of the prism (base of the prism), as shown in Fig. E.7.

Another prism used in spectroscopy is the Pellin–Broca prism. The operating principle of this prism can be understood as a variant of an equilateral prism ($\beta = \alpha = 60°$ in Fig. E.7).

Suppose that in the equilateral prism of Fig. E.8(a) a ray of a given wavelength is incident at the condition of least deviation (the ray refracted in the prism is parallel to the base). If the equilateral prism is separated into two prisms of 30° – 60° – 90°, as in Fig. E.8(b), the refracted ray still satisfies the

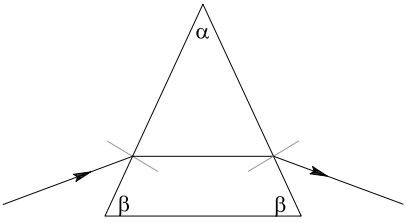

Figure E.7 An isosceles prism in which the minimum deviation of the ray occurs when the ray refracted within the prism propagates parallel to the base prism.

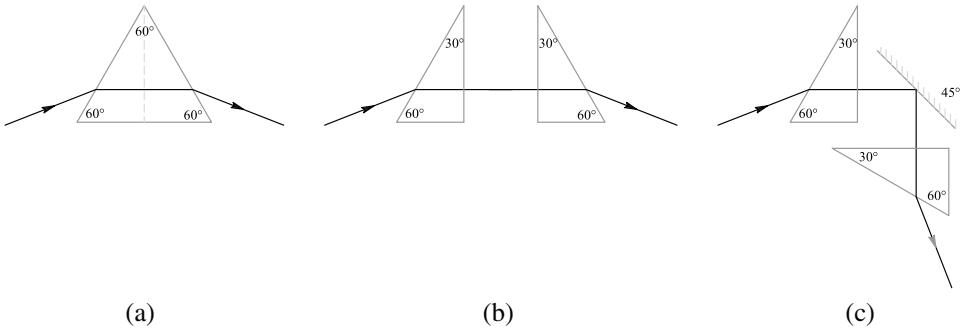

Figure E.8 Pellin–Broca prism principle. (a) Equilateral prism and a ray in condition of minimum deviation. (b) Separation of the equilateral prism into two prisms of 30° – 60° – 90° maintaining the condition of minimum deviation. (c) Change of the path of the ray by a mirror at 45° maintaining the condition of minimum deviation in the prisms. The end result is that the refracted ray makes an angle of 90° with the incident ray.

minimum deviation condition. If additionally a mirror is placed at 45° and the second prism is moved, as shown in Fig. E.8(c), the minimum deviation condition in the second prism still holds. The end result is that if the minimum deviation condition is met, the refracted beam, regardless of wavelength, will refract at an angle of 90° with respect to the incident ray.

If a 45° – 45° – 90° prism is used instead of the mirror, a prism like the one shown in Fig. E.9 can be created. This is the Pellin–Broca prism [3].

Thus, for a polychromatic incident ray, the ray refracted at 90° corresponds to a given wavelength. Rays of other wavelengths do not propagate under the minimum deviation condition and emerge from the prism at an angle other than 90°. However, with a small tilt around an axis orthogonal to the plane of the paper, the minimum deviation condition can be adjusted for another wavelength. In particular, if the axis of rotation passes through a point defined by the intersection of the angle bisector $\angle BAD$ and the side BC, i.e., point O in Fig. E.9, the ray refracted at 90° with respect to the incident ray maintains its lateral position.

This situation is illustrated in Fig. E.10 for two rays of different wavelengths in a prism whose indices of refraction for the two wavelengths are

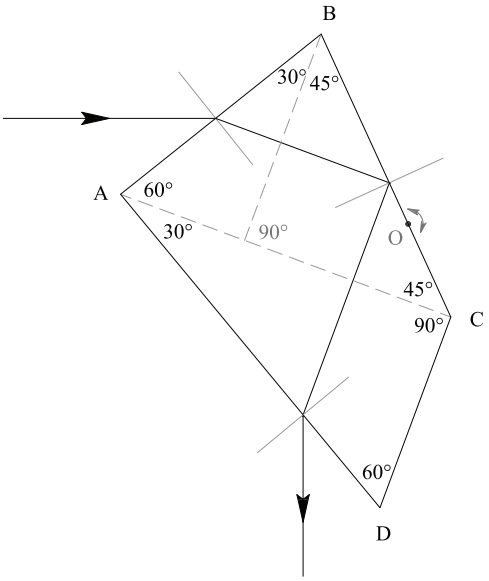

Figure E.9 Pellin–Broca prism.

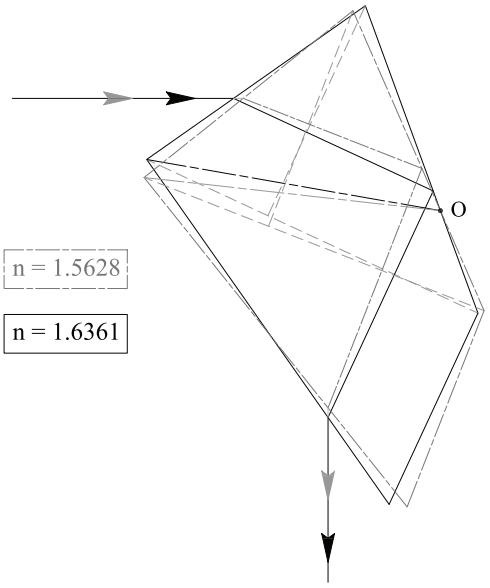

Figure E.10 Illustration of the advantage of rotating the prism at point O. Regardless of the wavelength, the ray refracted at 90° maintains its lateral position.

1.5628 and 1.6361. In Fig. E.10, there is an overlay of the prism with the two orientations (with the axis of rotation at O) that satisfy the minimum deviation condition for each wavelength. The orientation corresponding to the refractive index 1.5628 is shown in gray, and the orientation corresponding to

the refractive index 1.6361 is shown in black. The tilt angle is 3.5°. Indeed, the two refracted rays maintain their spatial location thanks to the rotation of the prism at point O. If it rotates at another point, the two rays are refracted with a lateral offset from each other. Thus, the pivot point at O offers an advantage when designing a spectrometer.

References

[1] Navel Education and Training Program Development Center, *Basic Optics and Optical Instruments*, Dover Publications, Mineola, New York (1997).

[2] E. Hecht, *Optics*, Global Edition, 5th ed., Pearson, Harlow, England (2017).

[3] P. Pellin and A. Broca, "A spectroscope of fixed deviation" *Apj* **10**, 337 (1899).

Appendix F
Polarization Ellipse

To determine the general polarization state, let us consider the real part of the amplitudes of the electric vector given in Eq. (2.31), i.e.,

$$E_x = |E_{ox}| \cos \delta_x, \tag{F.1}$$

$$E_y = |E_{oy}| \cos \delta_y. \tag{F.2}$$

Multiplying by $\sin \delta_x$ and $\sin \delta_y$ the functions $\cos \delta_x$ and $\cos \delta_y$ from Eqs. (F.1) and (F.2), as follows

$$\frac{E_x}{|E_{ox}|} \sin \delta_y = \cos \delta_x \sin \delta_y, \tag{F.3}$$

$$\frac{E_y}{|E_{oy}|} \sin \delta_x = \cos \delta_y \sin \delta_x, \tag{F.4}$$

and then subtracting Eq. (F.4) from Eq. (F.3) leads to

$$\frac{E_x}{|E_{ox}|} \sin \delta_y - \frac{E_y}{|E_{oy}|} \sin \delta_x = \sin(\delta_y - \delta_x). \tag{F.5}$$

By an analogous procedure, multiplying by $\cos \delta_x$ and $\cos \delta_y$ the functions $\cos \delta_x$ and $\cos \delta_y$ of Eqs. (F.1) and (F.2), and then subtracting, leads to

$$\frac{E_x}{|E_{ox}|} \cos \delta_y - \frac{E_y}{|E_{oy}|} \cos \delta_x = 0. \tag{F.6}$$

Finally, squaring Eqs. (F.5) and (F.6), and then adding them, leads to

$$\frac{E_x^2}{|E_{ox}|^2} - 2 \frac{E_x}{|E_{ox}|} \frac{E_y}{|E_{oy}|} \cos(\Delta\delta) + \frac{E_y^2}{|E_{oy}|^2} = \sin^2(\Delta\delta), \tag{F.7}$$

with $\Delta\delta = \delta_y - \delta_x$. This equation represents a rotated conic.* By rotating the axes, the crossed term of $E_x E_y$ is eliminated. The angle of rotation is

$$\tan 2\psi = -\frac{2\cos(\Delta\delta)/(|E_{ox}||E_{oy}|)}{1/|E_{ox}|^2 - 1/|E_{oy}|^2}. \tag{F.8}$$

By defining

$$\tan\alpha = \frac{|E_{oy}|}{|E_{ox}|}, \tag{F.9}$$

then

$$\tan 2\psi = \tan 2\alpha \cos\Delta\delta. \tag{F.10}$$

The sign of the discriminant of Eq. (F.7),

$$\cos^2(\Delta\delta)/(|E_{ox}||E_{oy}|)^2 - 1/(|E_{ox}||E_{oy}|)^2 = -\frac{\sin^2(\Delta\delta)}{(|E_{ox}||E_{oy}|)^2} < 0, \tag{F.11}$$

determines the type of conic. Because the result is less than zero, Eq. (F.7) is an ellipse rotated by the angle ψ in the Cartesian system xy.

*The quadratic form $Ax^2 + 2Bxy + Cy^2 = D$ represents a rotated conic in the Cartesian system xy. If $B^2 - AC < 0$, it is an ellipse; if $B^2 - AC = 0$, it is a parabola; if $B^2 - AC > 0$, it is a hyperbola. The unrotated version of the conic in a new Cartesian system $x'y'$ is achieved by a coordinate transformation corresponding to an eigenvalue problem of a symmetric matrix 2×2 whose elements are the coefficients A, B, and C. In the rotated coordinate system, the new coefficients are given by $A' = \frac{1}{2}[(A + C) + \sqrt{(A - C)^2 + 4B^2}]$, $C' = \frac{1}{2}[(A + C) - \sqrt{(A - C)^2 + 4B^2}]$; the angle of rotation can be determined from $\psi = \frac{1}{2}\arctan(\frac{2B}{A-C})$.